energies

MDPI

Article

Comparative Analysis of Material Efficiency and the Impact of Perforations on Heat Sinks for Monocrystalline Photovoltaic Panel Cooling

Raúl Cabrera-Escobar [1], José Cabrera-Escobar [2,*], David Vera [1], Francisco Jurado [1], Lenin Orozco-Cantos [2], Manolo Córdova-Suárez [2] and Félix García-Mora [3]

[1] Department of Electrical Engineering, Universidad de Jaén, 23071 Jaén, Spain
[2] Faculty of Engineering, Universidad Nacional de Chimborazo, Riobamba 060110, Ecuador
[3] Faculty of Mechanics, Escuela Superior Politécnica de Chimborazo (ESPOCH), Riobamba 060155, Ecuador
* Correspondence: omar.cabrera@unach.edu.ec

Abstract: In this research, the design and simulation of a heat sink for photovoltaic panels were carried out using aluminum and copper, the most commonly used materials in heat dissipation systems. This heat sink consisted of fins that were tested both perforated and non-perforated to improve heat dissipation efficiency. This research stems from the need to reduce the temperature of photovoltaic panels during operation, as scientific evidence shows that photovoltaic panels experience a decrease in efficiency as the temperature increases, taking as a reference the temperature under standard test conditions. The simulations of photovoltaic panels with aluminum and copper fins, both perforated and non-perforated, followed a rigorous methodology. For validation, the simulation results were compared with field data, yielding a mean absolute percentage error of 1.71%. The findings indicate that copper fins reduced the temperature of the photovoltaic panel by 2.62 K, resulting in a 1.31% increase in efficiency. Similarly, aluminum fins reduced the temperature by 2.10 K, with a 1.05% increase in efficiency. Perforated copper fins achieved a temperature reduction of 3.07 K, increasing efficiency by 1.54%, while perforated aluminum fins reduced the temperature by 2.49 K, contributing to a 1.25% increase in efficiency.

Keywords: heat dissipation; PV; heat fins; FEM; solar energy

check for updates

Citation: Cabrera-Escobar, R.; Cabrera-Escobar, J.; Vera, D.; Jurado, F.; Orozco-Cantos, L.; Córdova-Suárez, M.; García-Mora, F. Comparative Analysis of Material Efficiency and the Impact of Perforations on Heat Sinks for Monocrystalline Photovoltaic Panel Cooling. *Energies* **2024**, *17*, 5511. https://doi.org/10.3390/en17215511

Academic Editors: Maurizio Acciarri and Ignacio Mauleón

Received: 26 September 2024
Revised: 20 October 2024
Accepted: 31 October 2024
Published: 4 November 2024

Copyright: © 2024 by the authors. Licensee MDPI, Basel, Switzerland. This article is an open access article distributed under the terms and conditions of the Creative Commons Attribution (CC BY) license (https://creativecommons.org/licenses/by/4.0/).

1. Introduction

The global demand for energy is constantly increasing; concurrently, efforts to reduce greenhouse gas emissions have driven the adoption of renewable energy sources as a viable solution [1]. Solar photovoltaic technology is positioned as the leading innovation in sustainable energies, achieving the efficient conversion of solar radiation into electrical energy [2]. This technology facilitates a significant reduction in the dependency on fossil fuels and is crucial for mitigating climate change. The implementation of monocrystalline photovoltaic panels has experienced a remarkable increase in the conversion of solar energy into electricity [3], standing out for their superior efficiency compared to other photovoltaic technologies. However, during their operation, these panels can reach high temperatures [4], which can negatively affect their performance [5–7]. The conversion efficiency of photovoltaic panels, which indicates the percentage of sunlight converted into usable electrical energy, varies significantly, from 4% to 23%, depending on the type of solar cell used [8,9]. This is the percentage of solar energy that is utilized; the rest of the energy is lost as heat [10]. It has been estimated that a temperature increase of 1 K above STC in monocrystalline silicon cells results in a 0.5% decrease in electrical efficiency [11–14]; additionally, photovoltaic semiconductors can experience an increased degradation of up to 43% due to the rise in temperature [15]. Given these conditions, there is a need to develop effective cooling techniques. In this context, a simplified design of cooling fins for

monocrystalline photovoltaic panels is proposed, which not only reinforces the structure of the panel but also improves electrical efficiency, increasing energy production per unit area. To optimize this design, simulation through finite element analysis was employed.

The use of FEM in this field of research offers several advantages, making it an ideal tool for the thermal analysis of photovoltaic solar panels. Firstly, FEM enables the precise modeling of temperature distribution in the panels and heat dissipation fins under various operating conditions, as it divides the study domain into a mesh of discrete elements. This facilitates a detailed representation of heat transfer mechanisms, such as conduction, convection, and radiation, even in complex geometries like perforated fins. Additionally, FEM provides the flexibility to adjust the thermal properties of materials, boundary conditions, and system–environment interactions, which is crucial for simulating realistic scenarios and obtaining accurate results. Another significant advantage is its capability to perform parametric analysis, allowing for rapid evaluation of how changes in fin design affect the system's thermal efficiency. Furthermore, using FEM helps identify and optimize critical areas of heat dissipation, thereby reducing overheating and increasing the panels' electrical efficiency, without the need for costly and time-consuming experimental tests.

Various research efforts have been undertaken to understand the thermal behavior of photovoltaic panels. Among these, studies that use computational simulation tools via FEM stand out. A notable example in this area is the work by Moreno et al. [16], who conducted a comparison between closed-form solutions and finite element methods for heat transfer in a glass-free, nearly horizontal flat-plate water PVT collector. The performance of the PVT system with an 8° tilt was evaluated through simulations using FEM. To ensure the reliability of the results obtained, a mathematical validation model was implemented, allowing the correlation of simulation predictions with theoretical data.

In [17], a truncated, multi-level fin heat sink was developed to improve thermal dissipation in PV modules subjected to natural convection. An innovative heat sink was designed to induce abrupt changes in the boundary layer to enhance heat transfer, investigating the effects of fin spacing, height, and thickness using FEA. A parametric study was conducted comparing the proposed design with conventional rectangular fin heat sinks, varying parameters such as fin spacing (10–35 mm), height (60–120 mm), and thickness (0.5–1.5 mm). The results showed an average reduction in the PV module temperature by 6.13% and an improvement in power output by 2.87%, theoretically and experimentally validating the effectiveness of the proposed design for thermal management in photovoltaic systems.

Through FEM simulation, one study investigated a design for heat-dissipating fins made of copper integrated into monocrystalline photovoltaic panels to mitigate temperature increases during operation [18]. Photovoltaic panel simulations, with and without fins, were performed under standard and extreme conditions. The process encompassed design, meshing, model selection, boundary condition assignment, and validation, achieving a 0.28% mean absolute percentage error. Fins with a 40 mm height yielded the best heat dissipation, reducing panel temperature by 2.64 K and increasing efficiency by 1.32%, with improved performance at higher temperatures.

Advancements have been made in understanding the behavior of photovoltaic panels through the use of CFD. Among these studies, the research conducted by [19] stands out. The study experimentally analyzed a passive cooling technique for photovoltaic panels, aiming to increase energy conversion efficiency by reducing the panel's operating temperature. Aluminum fins were mounted on the rear surface of a PV panel using conductive epoxy glue. Two specific fin configurations were considered to improve the cooling rate from the rear surface of the PV panel: parallel aluminum fins and randomly arranged perforated L-profiles. It was found that the second configuration, with perforated L-profiles, showed better performance, with an average improvement of 2% in efficiency relative to the total power output. The results showed that the passive cooling technique could increase the efficiency of PV systems and potentially extend the lifespan of the panels

by reducing their operating temperature. The results were obtained in November in the city of Split, Croatia.

In [20], a comparative study was conducted of the thermal performance of a heat sink with discontinuous fins for the passive cooling of photovoltaic modules using numerical simulations with CFD. The results showed a temperature reduction of up to 7 °C with the proposed design compared to a conventional continuous fin design. To validate these results, two prototypes were built, and experimental tests were conducted in a solar simulator, confirming an average temperature reduction of 5 °C and greater thermal homogeneity with the discontinuous fin design, which also improved hydraulic characteristics by reducing pressure losses by 49%. This design proved to be more suitable for larger-scale applications due to its more consistent thermal performance and lower pressure drop, which is significant for improving the efficiency and lifespan of photovoltaic modules, especially in hot climates with high solar irradiation.

Recent research has evaluated advanced cooling systems to enhance the efficiency of photovoltaic–thermal (PV-T) solar panels, such as the use of copper fins and variable air circulation to optimize heat transfer by increasing turbulence in the airflow. A particular study was conducted by Arslan et al. [21], who designed a PV-T system with perforated fins that varied in height from the inlet to the outlet of the collector, achieving a thermal efficiency of 32.71% and an electrical efficiency of 12.77%, with a 0.38% improvement in electrical efficiency due to air cooling. Validated through CFD analysis, this approach proved to be effective in improving both thermal and electrical generation, adding to other advancements in thermal management to increase solar panel performance and contribute to the development of more efficient and sustainable solar energy technologies.

Research has also been conducted where heat sinks were tested and their results were analyzed using ANN. For example, Ref. [22] experimentally analyzed and dynamically modeled a PV equipped with porous fins to improve its performance. Tests were conducted at Firat University, Turkey, measuring variables such as ambient temperature, back surface temperatures of the panels, current, voltage, radiation, and wind speed. The results showed that the addition of porous fins reduced the surface temperature of the panels and increased the power output, with a maximum power difference of 7.26 W observed at 11:00. Dynamic models based on artificial neural networks were developed, which demonstrated a high correlation between experimental and predicted data, indicating acceptable accuracy for predicting the performance of these systems.

In addition, Bayrak et al. [23] conducted experimental research and dynamic modeling of a photovoltaic module equipped with porous fins. Experiments were carried out using polycrystalline panels under clear sky conditions in Elazig, Turkey. Porous metal fins were integrated into the back of the photovoltaic module to evaluate their effect on the panel's efficiency. Variables such as ambient temperature, panel surface temperature, solar radiation, wind speed, current, and voltage were measured using a 40-channel data acquisition system. The experimental results were used to develop a dynamic mathematical model based on artificial neural networks to predict system performance and design controllers for future improvements.

Recent research has evaluated the use of advanced cooling systems to improve the efficiency of solar panels, which tend to lose performance due to the temperature increase during operation. A promising approach is the use of anodized heat sinks equipped with thermoelectric modules, which have been shown to effectively reduce the surface temperature of the panels and, consequently, improve their efficiency and power output. In a study by Salehi et al. [24], this type of system was observed to reduce the panel temperature by 10.04 °C, resulting in a 10.5% increase in both efficiency and generated power. These findings highlight the importance of implementing thermal management solutions in solar panels, as they help mitigate overheating, increase electrical performance, and extend the panels' lifespan.

In another study by Khanam et al. [25], a comparative analysis was conducted on the performance of different photovoltaic modules in four climatic zones of India. The

study evaluated monocrystalline silicon, polycrystalline silicon, and thin-film modules, finding that electrical efficiency significantly decreased at high module temperatures. However, modules with semi-transparent backplates showed higher efficiency compared to those with opaque backplates, as they allowed heat dissipation through uncovered areas, reducing the module's temperature and improving its performance.

Additionally, in a study by Firoozzadeh et al. [26], the use of aluminum fins, both in straight and zigzag configurations, mounted on the back of photovoltaic modules was investigated to improve heat transfer and, therefore, electrical efficiency. An experimental study conducted with modules equipped with 10 to 40 fins in different configurations found that zigzag fins reduced the temperature by up to 15 °C, resulting in a 13.7% increase in efficiency. This type of passive cooling proved to be an effective and economical solution to improve the performance of photovoltaic modules, highlighting the potential of integrating different fin geometries to maximize heat dissipation and enhance power generation.

In the reviewed studies employing FEM, CFD, and ANN simulations, there is a trend toward reducing the operating temperature of PV systems by using cooling systems based on natural and forced convection. While research has been conducted with fins, there has not been an analysis of the impact that the materials used in their construction have on heat dissipation efficiency, nor has the impact of perforations in the fins been analyzed. Therefore, this research conducts a comparative analysis of the efficiency of fins using copper and aluminum, which are commonly used materials for these purposes, and studies the impact of perforations on the efficiency of the fins.

2. Materials and Methods

In this study, the photovoltaic solar panels used were located at the National University of Chimborazo, as shown in Figure 1. Each panel consisted of 144 photovoltaic cells, with an individual area of 0.0162 m^2, facilitating the conversion of solar energy into electricity. These panels were subject to significant thermal variations during operation, which affected their efficiency, making the implementation of effective cooling systems crucial to optimize their performance.



Figure 1. PV in the field [18].

To ensure the validity of the simulation, it was essential to obtain accurate data on the environmental conditions and operating temperatures of the photovoltaic solar panels. For this purpose, an Ambient Weather WS-5000 (Chandler, AZ, USA) weather station, shown in Figure 2, was used to monitor key climatic variables such as solar irradiance,

ambient temperature, and wind speed. Simultaneously, temperature measurements of the photovoltaic panels were taken using a FLIR C5 (Wilsonville, OR, USA) thermal camera, which provided detailed thermal mapping, and a FLUKE 62 MAX (Washington, DC, USA) pyrometer for more precise point temperature measurement. These instruments, shown in Figure 3, ensured the comprehensive monitoring of the thermal conditions required to validate the simulation results.



Figure 2. Weather station.



Figure 3. Thermal camera and pyrometer.

In the context of this research, a detailed estimation of experimental uncertainty was carried out using the Gauss error propagation law. This method is essential for ensuring result accuracy, as it allows for the evaluation of how the uncertainty of directly measured variables is transmitted to those obtained indirectly. Equation (1) served as the basis for this analysis, providing a mathematical tool to quantify the accumulated uncertainty based on the individual uncertainties of each direct variable. By applying this approach, it was possible to not only determine the total uncertainty magnitude in the measurements but also identify the most significant factors affecting the quality of the experimental results [27].

$$W_R = \left[\left(\frac{\partial R}{\partial x_1} W_1 \right)^2 + \left(\frac{\partial R}{\partial x_2} W_2 \right)^2 + \ldots + \left(\frac{\partial R}{\partial x_n} W_n \right)^2 \right]^{\frac{1}{2}} \quad (1)$$

Table 1 presents the analysis of the accuracy of the measurement instruments used in the research, which were necessary to obtain the data for the validation of the simulation.

Table 1. Evaluation of the experimental accuracy of the instruments used in the experiment [18].

Equipment	Parameter	Accuracy	Industry Brand	Uncertainty Value	Range
Weather Station WS-5000	Solar Irradiance	±15%	Ambient Weather	0.001 W/m^2	0 to 2367.798 W/m^2
	Ambient Temperature	±2 °F	Ambient Weather	0.1 °F	−40 to 149 °F
	Ambient Humidity	±5%	Ambient Weather	1%	10 to 99%
Pyrometer 62 MAX	Temperature	1.0%	FLUKE	0.2 °F	−22 to 1202 °F
Thermographic Camera C5	Temperature	±5.5 °F	FLIR	1 °F	32 to 212 °F

Boundary conditions define how the different surfaces of a photovoltaic panel and fins interact with their environment. Below, the specific conditions applied to model solar radiation and heat transfer by convection are described.

Top surface of the photovoltaic panel: This surface was considered to be directly exposed to solar radiation, modeled as a heat source in the form of uniform solar irradiance over the entire surface. The energy absorbed by the panel depended on the absorptivity of the material and the intensity of the solar radiation (W/m^2) and was simulated using the values corresponding to standard test conditions. Additionally, the solar irradiance data obtained from the weather station, shown in Figure 4, were used. It was assumed that radiation losses to the environment were negligible, as most of the energy was dissipated through convection and conduction mechanisms.

Bottom surface of the photovoltaic panel: In this area, the heat exchange with the environment was modeled through natural convection. A convective heat transfer coefficient was applied, which depended on atmospheric conditions (ambient temperature and air velocity). This boundary condition took into account the fact that the air circulating beneath the panel dissipated part of the accumulated heat. The convection coefficient used was calculated based on the Nusselt number for natural convection, adjusted according to the panel's average temperature and the surrounding air properties.

Surface of the heat-dissipating fins: The fins were designed to enhance heat transfer through either forced or natural convection, depending on the environment. In this case, a convection coefficient was used that varied according to the airflow velocity and the fin geometry (including the presence or absence of perforations). The fins were modeled as surfaces that transferred heat to the surrounding air, and the heat extracted from the photovoltaic panel gradually dissipated through them. For greater accuracy, the turbulence induced in the airflow around the perforated fins was considered, which improved the efficiency of heat dissipation.

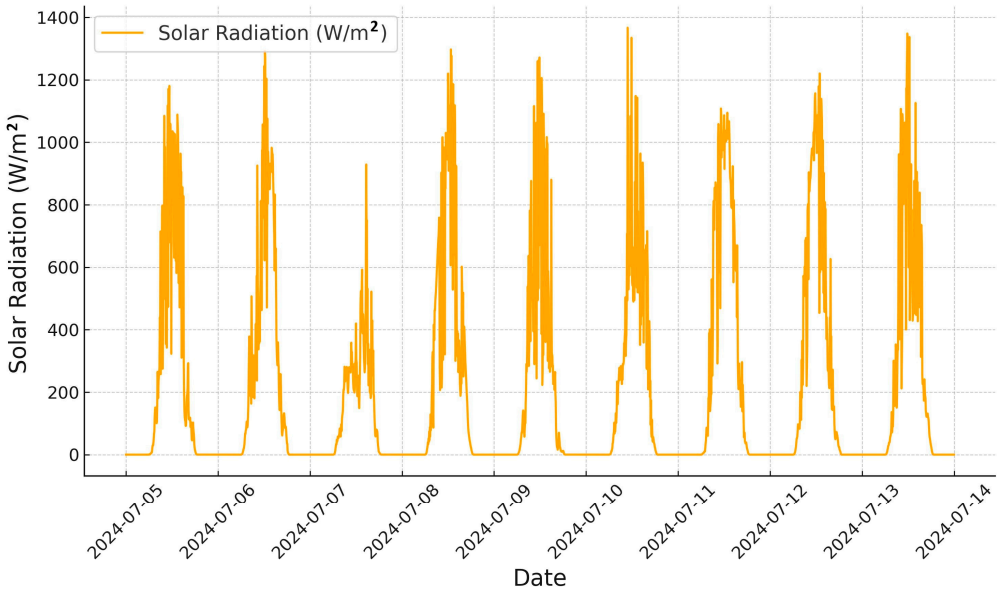


Figure 4. Solar irradiance.

Figures 4–6 show the curves of solar irradiance, ambient temperature, and air speed, respectively, that were used in this research. These climatic data were collected at the facilities of the Universidad Nacional de Chimborazo from 5 July to 13 July 2024, during a continuous 24 h period each day. These conditions were used to simulate the behavior of a photovoltaic module, providing an accurate and realistic framework for the analysis and dynamic modeling of the system.

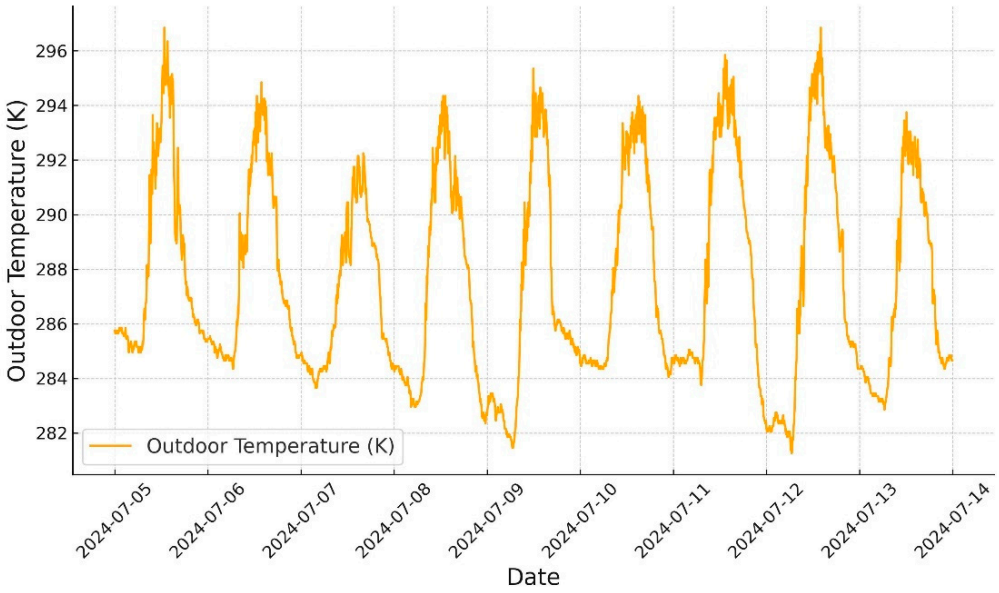


Figure 5. Ambient temperature.

The fins used in the simulations were made of copper and aluminum, both with and without perforations. These materials were chosen due to their high thermal conductivity, which aided in the dissipation of heat in the photovoltaic panel. The height of the fins was 40 mm, which was found to be the optimal height in the research by [18]. In Figure 7, the fins used, both with and without perforations, can be observed, with their dimensions.

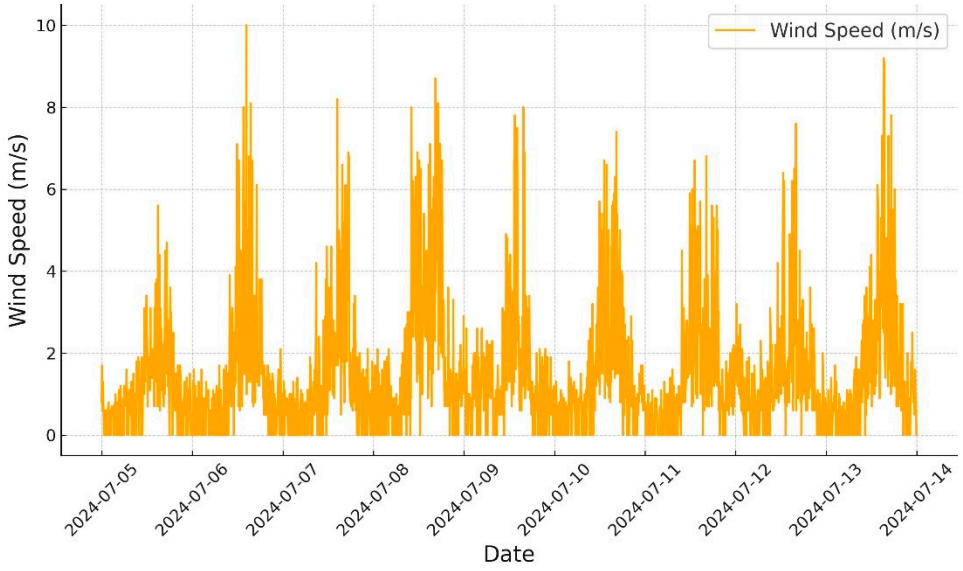


Figure 6. Wind speed.

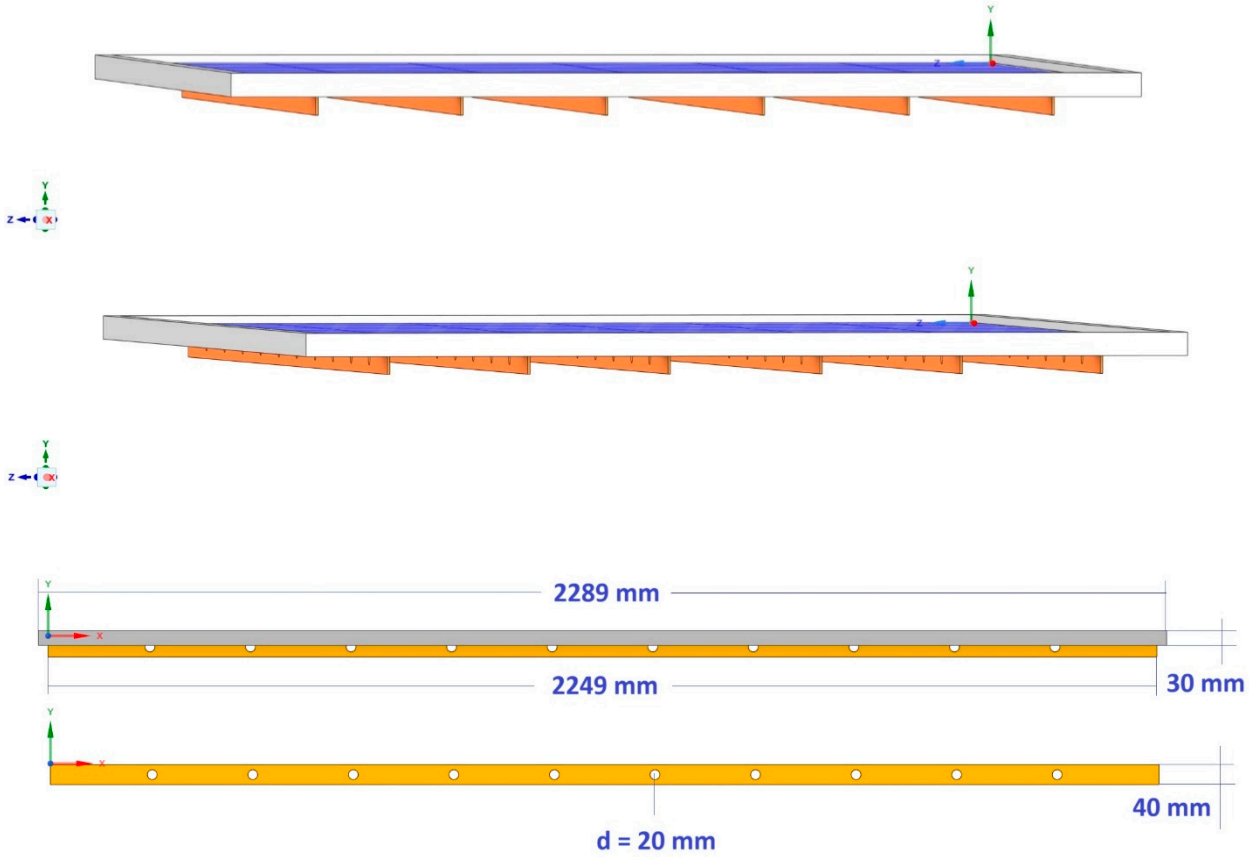


Figure 7. Fins without perforations and with perforations.

The simulation was conducted using the Steady-State Thermal module of Ansys Workbench. The process began with the creation of the prototype model in Ansys SpaceClaim 2023 R1, maintaining the same dimensions as the original design, as shown in Figure 8. The materials used in the construction of the prototype and their thermal properties are specified in Table 2.

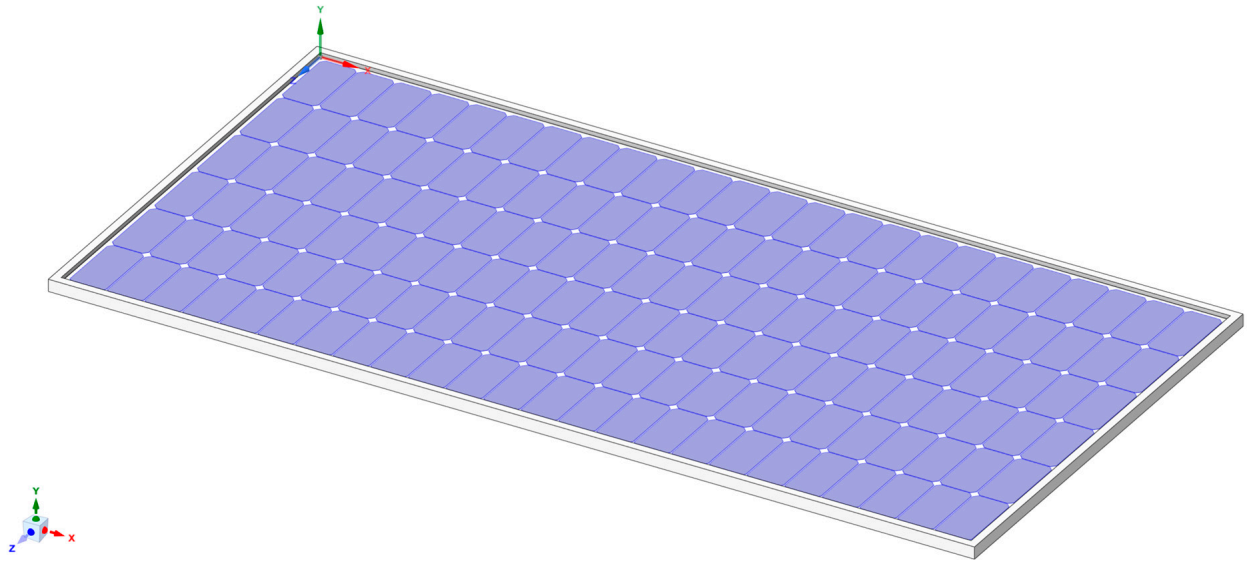


Figure 8. PV prototype design.

Table 2. Thermo-physical properties of the materials.

Materials	Thickness (mm)	Density (kg/m^3)	Thermal Conductivity (W/(m·K))	Specific Heat (J/(kg·K))
Glass	3	3000	1.8	5000
EVA	0.5	945	0.35	2090
Tedlar	0.1	1200	0.2	1250
Silicon	0.3	2330	148	700
Aluminum	0.71	2689	237.5	951
Copper	3	8933	400	385

The photovoltaic module consisted of multiple layers of different materials, each performing specialized functions. The glass layer optimized light transmission to increase energy efficiency, provided high resistance to environmental and chemical degradation, and allowed for lightweight and flexible configurations. This adaptability made it suitable for a wide range of applications and operational conditions [28]. The EVA layers functioned as encapsulating material for the solar cells, offering protection against environmental factors and ensuring their electrical insulation [29]. Tedlar provided protection against weather, ultraviolet radiation, electrical insulation, and structural durability; it acted as a barrier against moisture, rain, and other adverse climatic factors, preventing corrosion and deterioration of the internal components of the panel. Aluminum was used in the panel frames due to its lightness and corrosion resistance, ensuring structural stability. Both aluminum and copper were employed for the heat dissipation fins due to their high thermal conductivity, which improved heat dissipation and maintained panel efficiency.

The simulation, which began with the initial stages of designing the prototype and assigning the materials, continued with the discretization process [30]. The mesh used was of high quality with minimal distortion (average of 0.016309 and a maximum of 0.51209), indicating that the elements were well shaped. There were 1,306,288 nodes and 181,650 elements. The elements predominantly in the mesh were hexahedral. The metric used to evaluate the quality of this mesh was the Aspect Ratio [31], which indicated the proportionality and geometric uniformity of the elements that made up the mesh. The higher the quality of the mesh, the better the results obtained. The meshed PV used in this study can be seen in Figure 9.

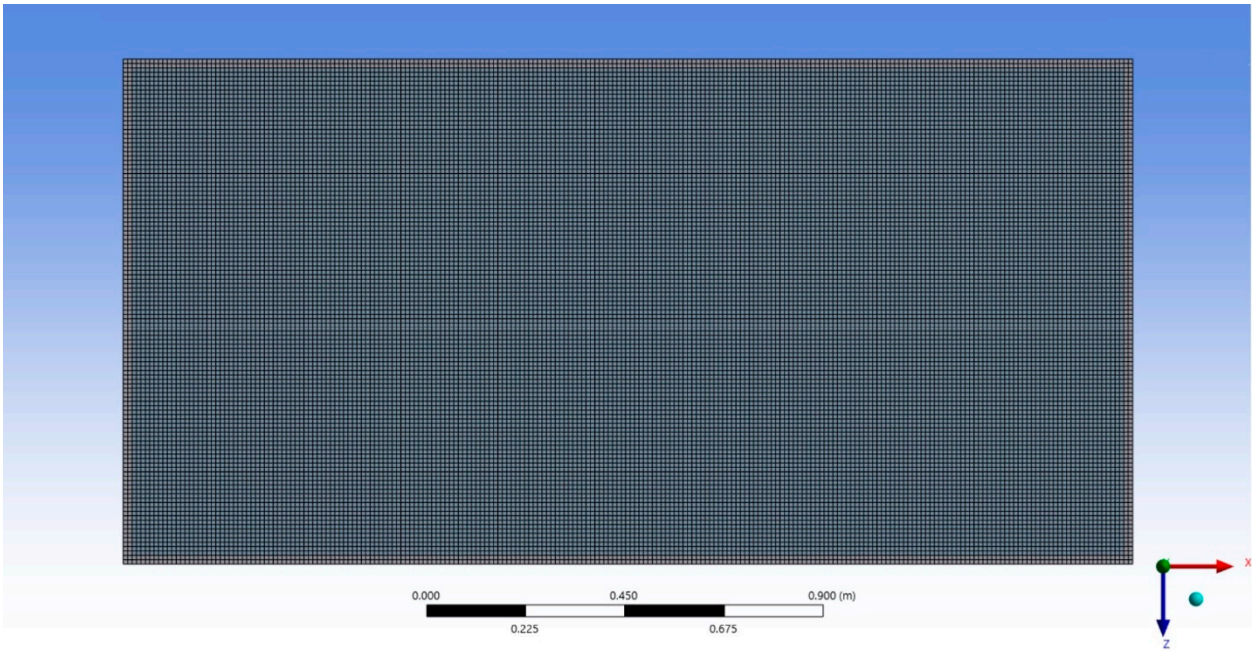


Figure 9. Meshing of the prototype.

For this research, FEM simulation was used to analyze the effects of heat transfer. This tool determined the temperature profiles of the PV under different conditions. FEM was used because no significant changes were observed in the flows in contact with the PV. If more details about the airflow around the PV had been desired, CFD would have been used [32], as was done in the study of a PVT where the flow of air and water was of interest [33]. The methodology used was based on the discretization of the study domain, in this case, the prototype, into a set of finite elements [34].

For the steady-state thermal analysis, the energy equation was used, which states that the sum of all the rates of heat entering and leaving a system must be zero, as can be seen in Equation (2).

$$\nabla \cdot (\kappa \nabla T) + q = 0 \tag{2}$$

Heat conduction through the materials of the PV module is described by Fourier's law, as shown in Equation (3).

$$q_{cond} = -\kappa \nabla T \tag{3}$$

The heat transfer by convection between the surface of a PV module and the environment is described by Newton's law of cooling, as shown in Equation (4).

$$q_{conv} = h(T_s - T_a) \tag{4}$$

The heat transfer by radiation between the surface of a PV module and the environment is described by the Stefan–Boltzmann law, as shown in Equation (5).

$$q_{rad} = \epsilon \sigma \left(T_s^4 - T_a^4 \right) \tag{5}$$

The energy balance for a PV module exposed to solar radiation is described by Equation (6).

$$q_{solar} = q_{cond} + q_{conv} + q_{rad} \tag{6}$$

Equation (7) was used to calculate the absorbed solar radiation.

$$q_{solar} = \alpha I \tag{7}$$

For the calculation of the convective coefficient, a mixed convective coefficient was used, as it was important to consider the effects of both natural and forced convection. To achieve this, the Nusselt number for forced and natural convection was calculated, as shown in Equations (8) and (9), respectively.

$$Nu_{forced} = 0.023 Re^{0.8} Pr^{0.3} \tag{8}$$

$$Nu_{natural} = CRa^{n} \tag{9}$$

From the calculation of the Nusselt number for forced and natural convection, a combined Nusselt number was determined, as shown in Equation (10).

$$Nu_{mixed} = \left(Nu_{forced}^{3} + Nu_{natural}^{3} \right)^{1/3} \tag{10}$$

Finally, the convective coefficient was determined using Equation (11).

$$h = \frac{Nu_{mixed} k_f}{L} \tag{11}$$

In the FEM simulation, the following assumptions were considered for simplicity:

- The materials used in the PV have properties that do not vary with temperature [35].
- Dust and partial shading have no effect on the analysis.
- The thermal contact between the elements of the PV is considered ideal.
- It operates in a steady state [36].
- The materials used in the construction of the PV have isotropic properties.
- The top surface of the PV is exposed to solar radiation.

3. Results and Discussion

Validation was performed by comparing the in situ temperature measurements on the photovoltaic panels at the National University of Chimborazo with the data obtained through simulation. To quantify the accuracy of the simulated data compared to the real data, the MAPE was calculated using Equation (12), which confirmed that the simulation results provided a good approximation of the real conditions [36].

$$MAPE = \frac{1}{n} \sum_{i=1}^{n} \left| \frac{A_i - F_i}{A_i} \right| \times 100\% \tag{12}$$

By conducting a comparative analysis between the real data obtained through experimental measurements and the data acquired through FEM simulation, a MAPE of 1.71% was determined, indicating a high correlation between the real data obtained from experimental measurements and the data acquired through FEM simulation. Figure 10, presents the temperature distribution of the PV under Riobamba's atmospheric conditions obtained through simulation. Figure 11 shows the temperature distribution of the PV obtained using the thermal camera.

Once the employed methodology had been validated, the simulations of the photovoltaic solar panel equipped with copper and aluminum fins, both perforated and non-perforated, were conducted. The simulations were performed under STC conditions (temperature of 298.15 K and solar irradiance of 1000 W/m^2). Figure 12 shows the temperature distribution under STC conditions for the photovoltaic panel without fins. The maximum, minimum, and average temperatures were 330.26, 306.28, and 326.09 K, respectively. The panel had a thermal fluctuation of 23.46 K. These data served as a reference for comparison with the different configurations that were used for the heat dissipators.

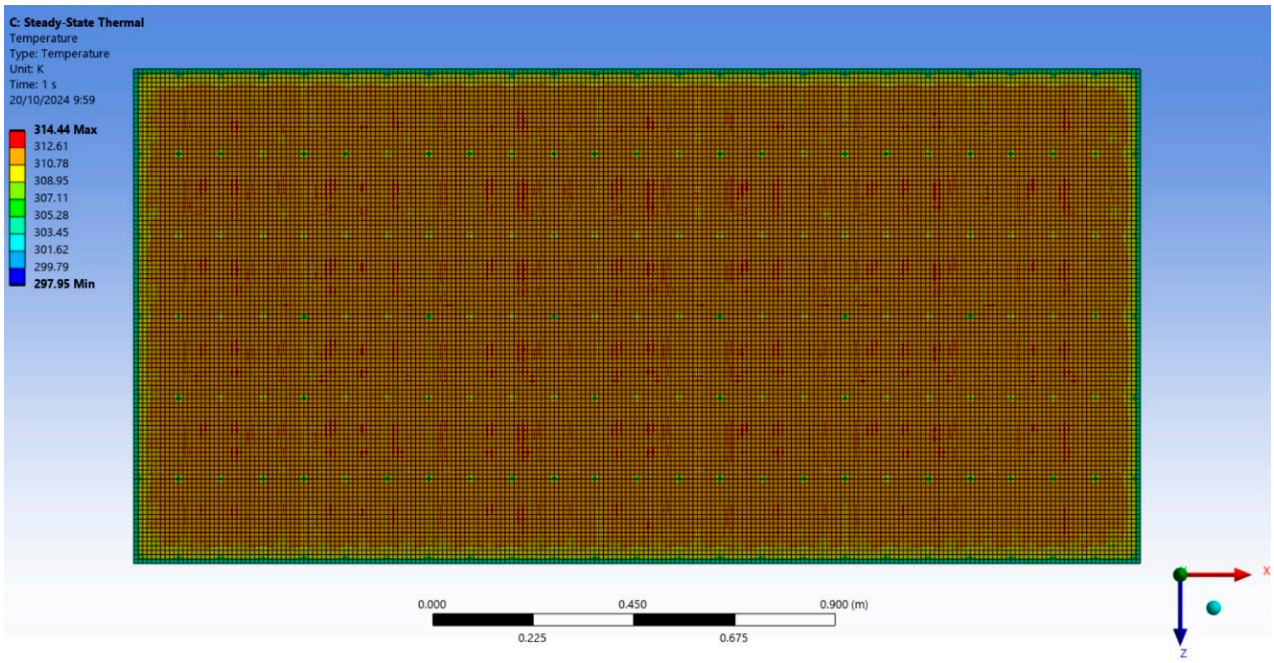


Figure 10. Temperature distribution obtained through simulation using the specific atmospheric conditions of the city of Riobamba.

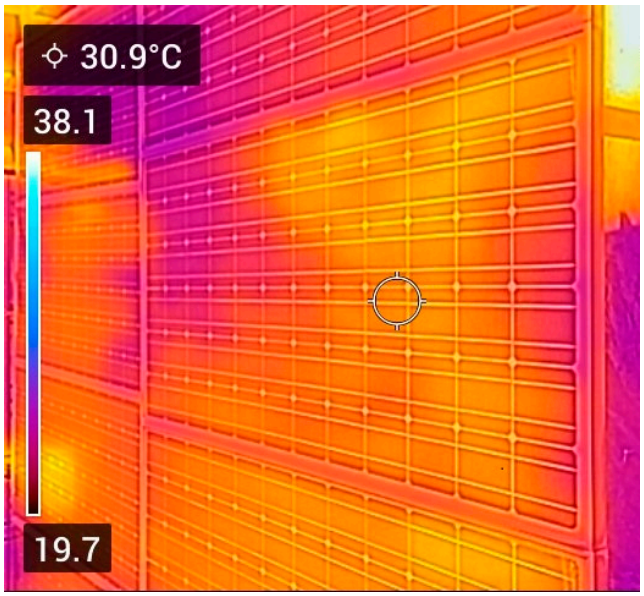


Figure 11. Temperature distribution obtained experimentally using the specific atmospheric conditions of the city of Riobamba.

Figure 13 shows the temperature distribution under STC conditions for the photovoltaic panel with non-perforated copper fins. The maximum, minimum, and average temperatures were 327.81, 304.43, and 323.45 K, respectively, and the panel had a thermal fluctuation of 23.38 K. The temperature distribution showed that while a notable reduction in the maximum temperature of the panel was achieved compared to the panel without fins, heat dissipation was more homogeneous in the regions near the fins. However, there were areas with significant thermal differences that could indicate limited heat flow due to natural convection without the assistance of additional turbulence.

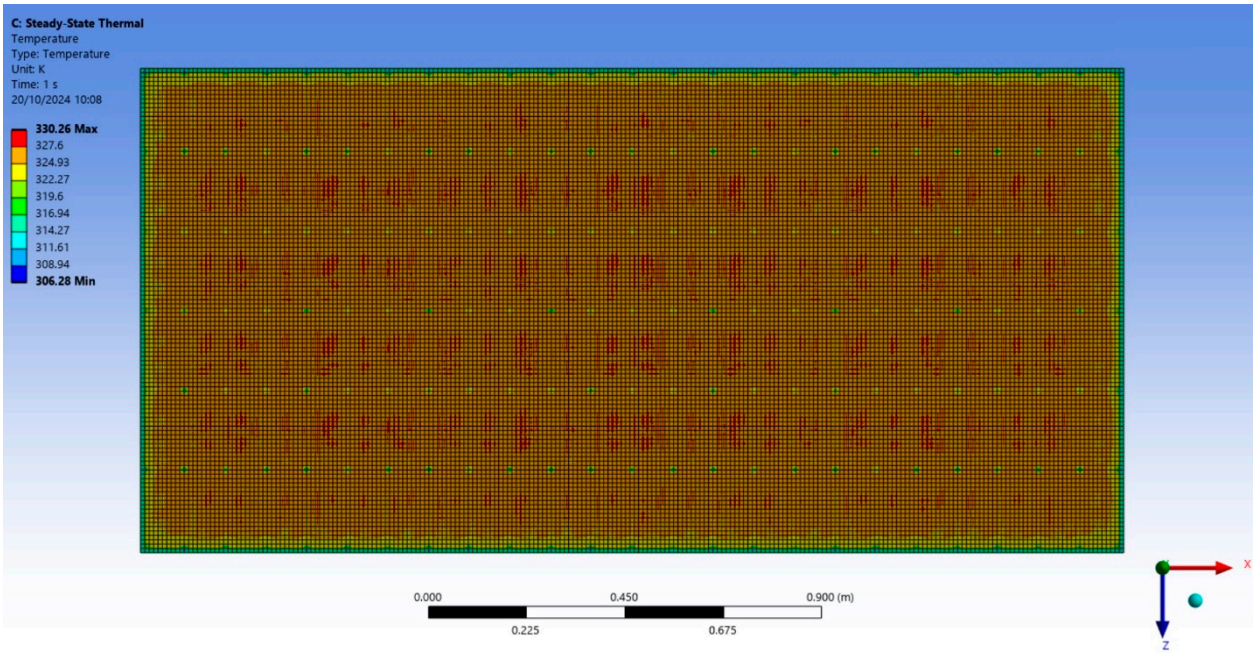


Figure 12. Temperature distribution of the modeled photovoltaic panel without fins under standard test conditions.

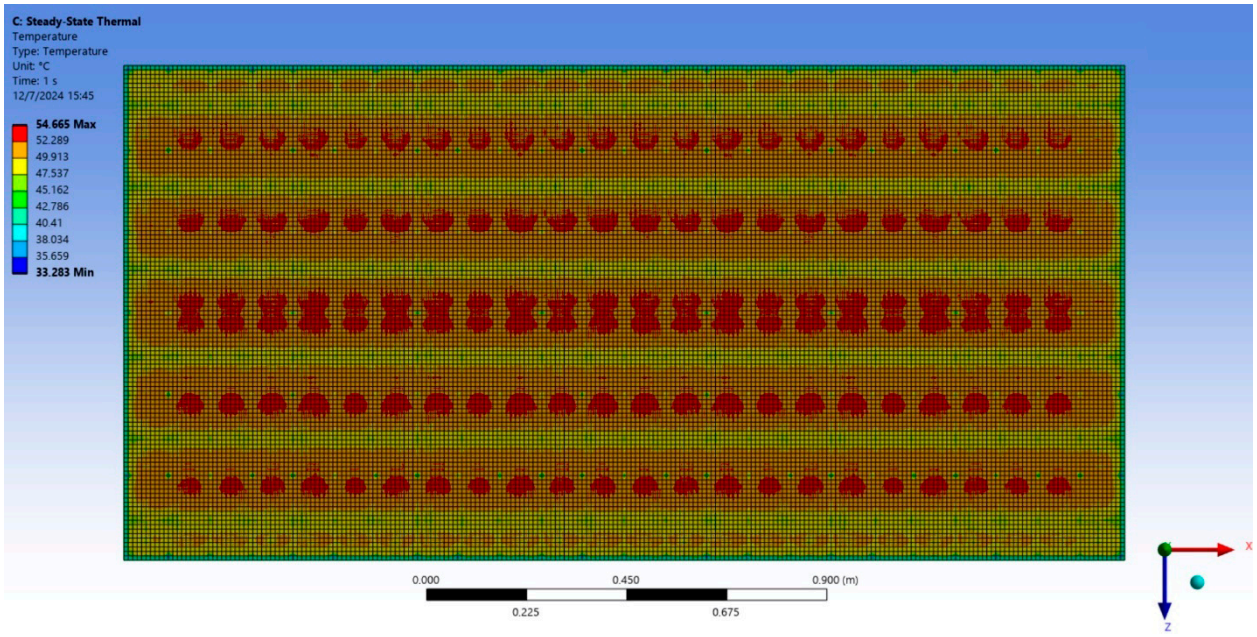


Figure 13. Temperature distribution of the photovoltaic panel with non-perforated copper fins.

Figure 14 shows the temperature distribution under STC conditions for the photovoltaic panel with non-perforated aluminum fins. The maximum, minimum, and average temperatures were 328.21, 306.40, and 323.97 K, respectively, and the panel had a thermal fluctuation of 21.81 K. In this configuration, a similar trend was observed, with an effective reduction in the panel's temperature, although aluminum's ability to dissipate heat was slightly lower than that of copper due to its lower thermal conductivity. Additionally, the temperature variation on the panel's surface was somewhat greater, suggesting that aluminum did not achieve thermal dissipation as uniformly as copper.

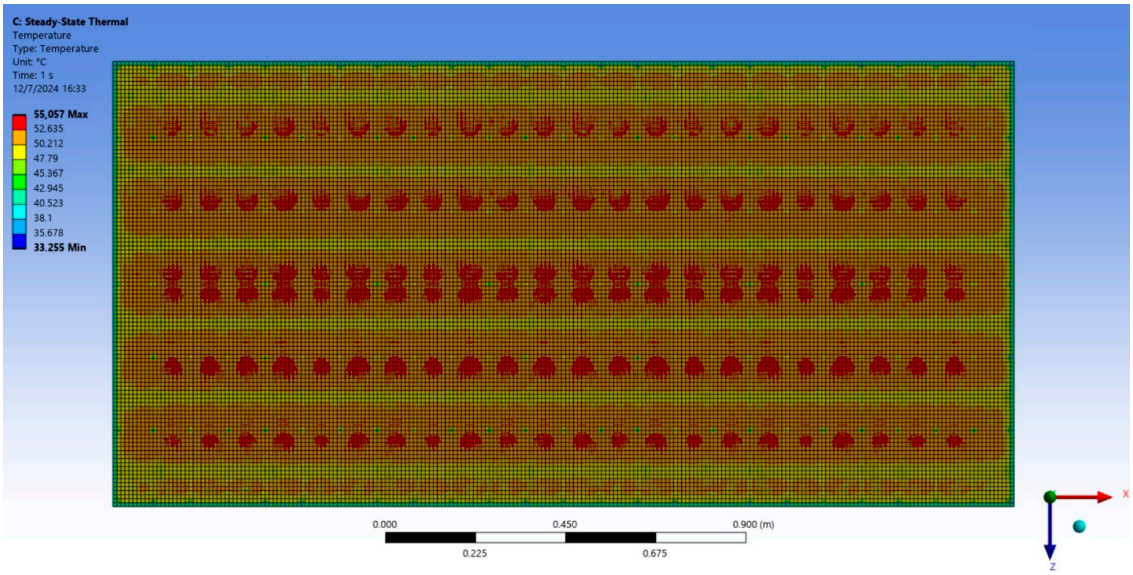


Figure 14. Temperature distribution of the photovoltaic panel with non-perforated aluminum fins.

Figure 15 shows the temperature distribution under STC conditions for the photovoltaic panel with perforated copper fins. The maximum, minimum, and average temperatures were 327.60, 306.46, and 323.00 K, respectively, and the panel had a thermal fluctuation of 21.14 K. The introduction of perforations in the copper fins generated a more uniform thermal distribution. The turbulence induced by the perforations enhanced convection and allowed for greater heat dissipation in the areas near the fins. An additional reduction in the panel's average temperature was observed, confirming that the perforations significantly increased the efficiency of the fins, not only by increasing the contact area with the air but also by improving the convective flow.

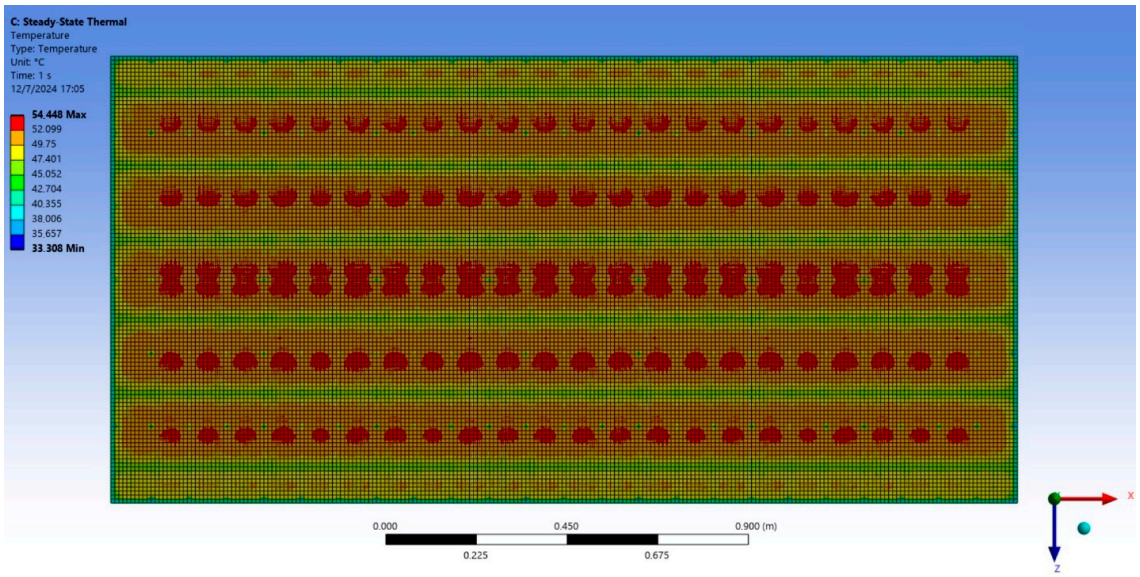


Figure 15. Temperature distribution of the photovoltaic panel with perforated copper fins.

Finally, Figure 16 shows the temperature distribution under STC conditions for the photovoltaic panel with perforated aluminum fins. The maximum, minimum, and average temperatures were 327.90, 306.53, and 323.58 K, respectively, and the panel had a thermal fluctuation of 21.37 K. Similar to the perforated copper configuration, the aluminum fins with perforations showed a more homogeneous temperature distribution compared to fins

without perforations. Although the temperature reduction was not as significant as in the case of copper, the addition of perforations improved air convection and reduced hot spots on the panel's surface.

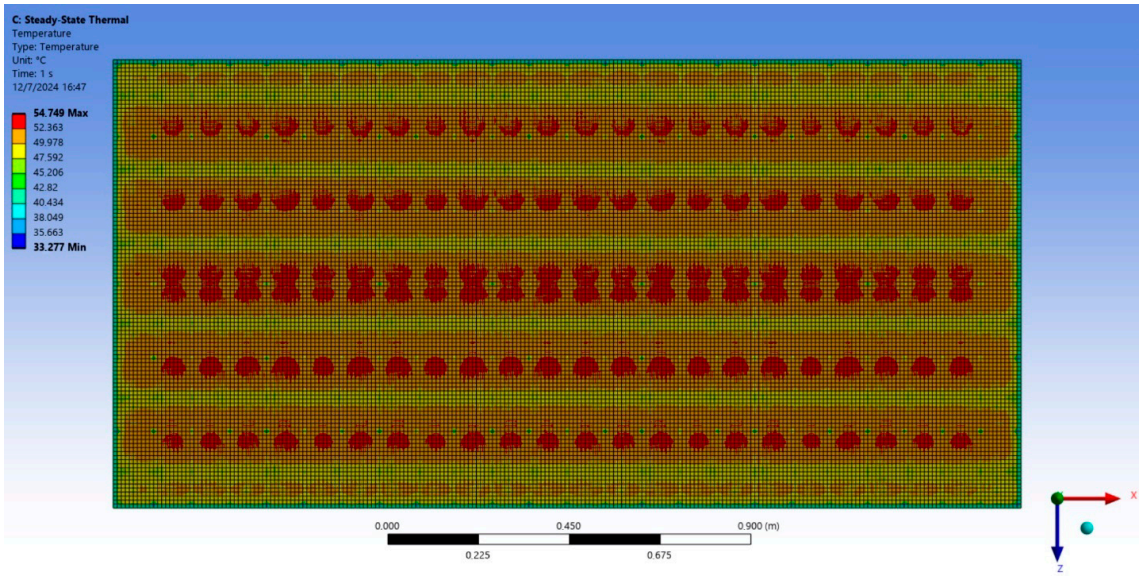


Figure 16. Temperature distribution of the photovoltaic panel with perforated aluminum fins.

Table 3 presents the temperatures of photovoltaic panels with copper and aluminum fins, both perforated and non-perforated. The PV with non-perforated copper fins had a temperature reduction of 2.62 K, resulting in a 1.31% increase in efficiency. The PV with non-perforated aluminum fins had a temperature reduction of 2.10 K, resulting in a 1.05% increase in efficiency. The PV with perforated copper fins had a temperature reduction of 3.07 K, resulting in a 1.54% increase in efficiency. The PV with perforated aluminum fins had a temperature reduction of 2.49 K, resulting in a 1.25% increase in efficiency.

Table 3. Photovoltaic panel temperatures.

Fins	Maximum Temperature (K)	Minimum Temperature (K)	Average Temperature (K)	Reducción de Temperatura (K)	Aumento de Eficiencia (%)
PV Without Fins	330.26	306.28	326.07	-	-
Non-Perforated Copper	327.81	304.43	323.45	2.62	1.31
Non-Perforated Aluminum	328.21	306.40	323.97	2.10	1.05
Perforated Copper	327.60	306.46	323.00	3.07	1.54
Perforated Aluminum	327.90	306.53	323.58	2.49	1.25

When comparing the thermal profile figures and analyzing Table 3, the following observations can be made:

Fin Material: Aluminum fins tended to have slightly higher maximum temperatures compared to copper fins, both in non-perforated (Figure 14) and perforated (Figure 16) configurations. Copper fins exhibited less temperature variation, which may indicate better thermal dissipation capacity.

Fin Design: Perforated fins (Figures 15 and 16) showed a more uniform thermal distribution compared to non-perforated fins (Figures 13 and 14). This suggests that perforations can help improve air circulation and heat dissipation. The minimum and average temperatures were closer together for the perforated fins, implying greater efficiency in thermal management.

Thermal Performance: The difference between the maximum and minimum temperatures for perforated copper fins was smaller than for aluminum fins, reaffirming the superiority of copper in thermal management. However, perforated aluminum fins also demonstrated good thermal dissipation capacity, which could be advantageous considering cost and weight factors.

The temperature reduction observed in configurations with perforated fins was due to not only increased contact between the photovoltaic panel and the environment but also significant changes in the airflow dynamics that these perforations generated. By perforating the fins, a more turbulent airflow was promoted around the surfaces of the heat sink, significantly increasing the efficiency of heat transfer through convection.

An analysis of the flow field showed that the perforations in the fins acted as disruptors of the laminar flow, allowing air to enter through the holes and generating vortices near the perforations. These disturbances induced a higher heat transfer coefficient due to an increase in the local Nusselt number, which, in turn, improved the thermal dissipation capacity of the fins. In comparison, fins without perforations showed a more uniform but less effective flow in terms of convection, as insufficient turbulence was generated to maximize heat transfer.

Additionally, the perforations not only increased the contact surface with the air but also allowed for better convective flow through the fins. This improved ventilation around the heat sink, reducing heat accumulation points and promoting more homogeneous cooling. The presence of these perforations created low-pressure zones that encouraged the circulation of fresh air through the holes, increasing the temperature gradient between the fins and the surrounding air, which enhanced cooling efficiency.

Quantitative analysis of the results indicated that the turbulence increase induced by the perforations generated a 10–15% increase on average in the convection coefficient compared to non-perforated fins. This phenomenon was consistent with the improvement observed in the temperature distribution in the simulations, where the perforated fins showed a smaller temperature difference between the upper and lower surfaces, indicating more efficient heat dissipation.

From a practical standpoint, these findings suggest that the use of perforated fins can optimize the design of passive cooling systems in photovoltaic panels, especially in conditions where natural convection is the primary mechanism of thermal dissipation. The turbulent flow induced by perforations not only improves cooling but also allows for a reduction in the material used to manufacture the fins, decreasing their weight and cost without compromising heat dissipation capacity.

4. Conclusions and Recommendations

A methodology based on the finite element method was developed to simulate a photovoltaic panel with heat-dissipation fins made of copper and aluminum. The objective was to evaluate the effectiveness of these fins in thermal dissipation, considering both perforated and non-perforated configurations. The simulation incorporated a detailed FEM analysis, allowing for precise characterization of the temperature profiles in the photovoltaic system under different operating conditions. The results showed that perforated copper fins achieved the greatest temperature reduction, with a decrease of 3.07 K, leading to a 1.54% increase in panel efficiency. This improvement is attributed to the increased surface contact with the air and the turbulence generated by the perforations, optimizing heat transfer by convection and reducing hot spots on the panel surface. This highlights the importance of the geometric characteristics and material of the fins in the design of cooling systems for solar panels, enhancing operational efficiency and extending the system's lifespan.

The fins generated a decrease in the temperature gradient, which favored the operation of the PV. These results were obtained with both copper and aluminum fins, with and without perforations, improving heat dissipation. This uniformity was crucial for minimizing hot spots and improving the operational efficiency and lifespan of the photovoltaic panel. Additionally, this study revealed that the areas with the highest temperatures were located

near the electrical connections, suggesting the need to optimize the design of the fins and the arrangement of the cells to further enhance thermal management.

From the analysis of the results, it can be observed that the perforations in the fins helped dissipate heat by adding additional surface area, which improved heat transfer to the environment. They also allowed air to flow through the fins, improving convection and even inducing turbulence in the airflow, which enhanced heat transfer due to better mixing of the air around the fins. An additional advantage of using perforations was that they reduced the mass of the fins without significantly compromising their heat dissipation capacity, which was beneficial as it reduced their weight.

The validation of the results obtained through simulation was performed by correlating them with empirical data collected by the weather station, thermal camera, and pyrometer. This validation process ensured that the simulated results were an accurate and reliable representation of real conditions.

Author Contributions: Methodology: R.C.-E., J.C.-E., D.V. and M.C.-S. Conceptualization: F.J., L.O.-C., M.C.-S. and F.G.-M. Investigation: J.C.-E., D.V., L.O.-C. and F.G.-M. Validation: R.C.-E. Software: J.C.-E. Formal analysis: D.V. Data curation: F.J. All authors have read and agreed to the published version of the manuscript.

Funding: This research received no external funding.

Data Availability Statement: Data are contained within the article.

Conflicts of Interest: The authors declare no conflicts of interest.

Nomenclature

A_i	Actual value for the ith observation
ANN	Artificial neural network
CFD	Computational fluid dynamics
EVA	Ethylene–vinyl acetate
FEA	Finite element analysis
FEM	Finite element method
F_i	Forecasted value for the ith observation
h	Convection heat transfer coefficient [W/m^2K]
I	Intensity of incident solar radiation [W/m^2]
k	Thermal conductivity [W/m.K]
L	Characteristic length [m]
MAPE	Mean absolute percentage error
n	Number of observations
Nu	Nusselt number
Nu_{mixed}	Mixed Nusselt number
Pr	Prandtl number
PV	Photovoltaic
PVT	Photovoltaic thermal
q	Heat source or sink [W/m^3]
q_{cond}	Rate of heat transfer by conduction [W/m^2]
q_{conv}	Rate of heat transfer by convection [W/m^2]
q_{rad}	Rate of heat transfer by radiation [W/m^2]
q_{solar}	Absorbed solar energy [W/m^2]
R	Uncertainty
Ra	Rayleigh number
Re	Reynolds number
STC	Standard test conditions
T	Temperature [K]
∇T	Temperature gradient [K/m]
W	Uncertainty of the independent variable
x	Independent variable

Greek letters

ρ	Density [kg/m^3]
σ	Stefan–Boltzman constant [W/m^{2}K^4]
$\in$	Surface emissivity
α	Absorption coefficient

Subscripts

s	Surface
a	Ambient
f	Fluid

References

1. Sen, C.; Kim, M.; Chen, D.; Varshney, U.; Liu, S.; Samadi, A.; Ciesla, A.; Wenham, S.R.; Chan, C.E.; Chong, C.; et al. Assessing the Impact of Thermal Profiles on the Elimination of Light- and Elevated-Temperature-Induced Degradation. *IEEE J. Photovoltaics* **2019**, *9*, 40–48. [CrossRef]
2. Charfi, W.; Chaabane, M.; Mhiri, H.; Bournot, P. Performance evaluation of a solar photovoltaic system. *Energy Rep.* **2018**, *4*, 400–406. [CrossRef]
3. Nižetić, S.; Jurčević, M.; Čoko, D.; Arıcı, M. A novel and effective passive cooling strategy for photovoltaic panel. *Renew. Sustain. Energy Rev.* **2021**, *145*, 111164. [CrossRef]
4. Cotfas, D.T.; Cotfas, P.A.; Machidon, O.M. Study of temperature coefficients for parameters of photovoltaic cells. *Int. J. Photoenergy* **2018**, *2018*, 5945602. [CrossRef]
5. Dhimish, M.; Holmes, V.; Mehrdadi, B.; Dales, M.; Mather, P. Output-power enhancement for hot spotted polycrystalline photovoltaic solar cells. *IEEE Trans. Device Mater. Reliab.* **2017**, *18*, 37–45. [CrossRef]
6. Hernandez-Perez, J.; Carrillo, J.; Bassam, A.; Flota-Banuelos, M.; Patino-Lopez, L. A new passive PV heatsink design to reduce efficiency losses: A computational and experimental evaluation. *Renew. Energy* **2020**, *147*, 1209–1220. [CrossRef]
7. Wang, J.-C.; Liao, M.-S.; Lee, Y.-C.; Liu, C.-Y.; Kuo, K.-C.; Chou, C.-Y.; Huang, C.-K.; Jiang, J.-A. On enhancing energy harvesting performance of the photovoltaic modules using an automatic cooling system and assessing its economic benefits of mitigating greenhouse effects on the environment. *J. Power Sources* **2018**, *376*, 55–65. [CrossRef]
8. IEA. *Technology Roadmap: Solar Photovoltaic Energy*; International Energy Agency: Paris, France, 2014.
9. de Wild-Scholten, M.J.M. Energy payback time and carbon footprint of commercial photovoltaic systems. *Sol. Energy Mater. Sol. Cells* **2013**, *119*, 296–305. [CrossRef]
10. Barukčić, M.; Ćorluka, V.; Miklošević, K. The irradiance and temperature dependent mathematical model for estimation of photovoltaic panel performances. *Energy Convers. Manag.* **2015**, *101*, 229–238. [CrossRef]
11. Kumar, M.; Kumar, A. Performance assessment and degradation analysis of solar photovoltaic technologies: A review. *Renew. Sustain. Energy Rev.* **2017**, *78*, 554–587. [CrossRef]
12. Chandrasekar, M.; Rajkumar, S.; Valavan, D. A review on the thermal regulation techniques for non integrated flat PV modules mounted on building top. *Energy Build.* **2015**, *86*, 692–697. [CrossRef]
13. Green, M.; Dunlop, E.; Hohl-Ebinger, J.; Yoshita, M.; Kopidakis, N.; Hao, X. Solar cell efficiency tables (version 57). *Prog. Photovolt. Res. Appl.* **2021**, *29*, 3–15. [CrossRef]
14. Ebaid, M.; Ghrair, A.; Al-Busoul, M. Experimental investigation of cooling photovoltaic (PV) panels using (TiO_2) nanofluid in water-polyethylene glycol mixture and (Al_2O_3) nanofluid in water- cetyltrimethylammonium bromide mixture. *Energy Convers. Manag.* **2018**, *155*, 324–343. [CrossRef]
15. Xu, P.; Zhang, X.; Shen, J.; Zhao, X.; He, W.; Li, D. Parallel experimental study of a novel super-thin thermal absorber based photovoltaic/thermal (PV/T) system against conventional photovoltaic (PV) system. *Energy Rep.* **2015**, *1*, 30–35. [CrossRef]
16. Moreno, D.; Fernández, M.; Esquivias, P.M. A comparison of closed-form and finite-element solutions for heat transfer in a nearly horizontal, unglazed flat plate PVT water collector: Performance assessment. *Sol. Energy* **2017**, *141*, 11–24. [CrossRef]
17. Ahmad, E.; Fazlizan, A.; Jarimi, H.; Sopian, K.; Ibrahim, A. Enhanced heat dissipation of truncated multi-level fin heat sink (MLFHS) in case of natural convection for photovoltaic cooling. *Case Stud. Therm. Eng.* **2021**, *28*, 101578. [CrossRef]
18. Cabrera-Escobar, R.; Vera, D.; Cabrera-Escobar, J.; Godoy, M.M.P.; Carrazco, D.C.; Llango, E.R.Z.; Jurado, F. Finite Element Analysis Method Design and Simulation of Fins for Cooling a Monocrystalline Photovoltaic Panel. *Clean Technol.* **2024**, *6*, 767–783. [CrossRef]
19. Grubišić-Čabo, F.; Nižetić, S.; Čoko, D.; Kragić, I.M.; Papadopoulos, A. Experimental investigation of the passive cooled free-standing photovoltaic panel with fixed aluminum fins on the backside surface. *J. Clean. Prod.* **2018**, *176*, 119–129. [CrossRef]
20. Hernandez-Perez, J.; Carrillo, J.; Bassam, A.; Flota-Banuelos, M.; Patino-Lopez, L. Thermal performance of a discontinuous finned heatsink profile for PV passive cooling. *Appl. Therm. Eng.* **2020**, *184*, 116238. [CrossRef]
21. Arslan, E.; Can, F.; Koşan, M.; Demirtaş, M.; Aktekeli, B.; Aktaş, M. Numerical and experimental assessment of a photovoltaic thermal collector using variable air volume. *Therm. Sci. Eng. Prog.* **2023**, *39*, 101735. [CrossRef]
22. Selimefendigil, F.; Bayrak, F.; Oztop, H.F. Experimental analysis and dynamic modeling of a photovoltaic module with porous fins. *Renew. Energy* **2018**, *125*, 193–205. [CrossRef]

23. Bayrak, F.; Oztop, H.F.; Selimefendigil, F. Effects of different fin parameters on temperature and efficiency for cooling of photovoltaic panels under natural convection. *Sol. Energy* **2019**, *188*, 484–494. [CrossRef]
24. Salehi, R.; Jahanbakhshi, A.; Golzarian, M.R.; Khojastehpour, M. Evaluation of solar panel cooling systems using anodized heat sink equipped with thermoelectric module through the parameters of temperature, power and efficiency. *Energy Convers. Manag. X* **2021**, *11*, 100102. [CrossRef]
25. Khanam, S.; Meraj; Azhar; Karimi, M.; Ahmad, T.; Arif, R.; Al-Kouz, W. Comparative performance analysis of photovoltaic modules of different materials for four different climatic zone of India. *Urban Clim.* **2021**, *39*, 100957. [CrossRef]
26. Firoozzadeh, M.; Shiravi, A.H.; Chandel, S.S. An experimental analysis of enhancing efficiency of photovoltaic modules using straight and zigzag fins. *J. Therm. Anal. Calorim.* **2022**, *147*, 8827–8839. [CrossRef]
27. Holman, J.P. *Experimental Methods for Engineers, (193) Americas*; McGraw Hill: New York, NY, USA, 2011.
28. Popovici, C.G.; Hudişteanu, S.V.; Mateescu, T.D.; Cherecheş, N.-C. Efficiency Improvement of Photovoltaic Panels by Using Air Cooled Heat Sinks. *Energy Procedia* **2016**, *85*, 425–432. [CrossRef]
29. Muhfidin, R.; Yu, S. Thermal Analysis of PV Module and the Effect on its Efficiency. In Proceedings of the 2019 International Conference on Technologies and Policies in Electric Power & Energy, Yogyakarta, Indonesia, 21–22 October 2019; pp. 1–4.
30. Cabrera-Escobar, J.; Vera, D.; Jurado, F.; Córdova-Suárez, M.; Santillán-Valdiviezo, G.; Rodríguez-Orta, A.; Cabrera-Escobar, R. Optimization of olive pomace dehydration process through the integration of computational fluid dynamics and deep learning. *Energy Sources Part A Recover. Util. Environ. Eff.* **2024**, *46*, 4756–4776. [CrossRef]
31. ANSYS, Inc. *Mechanical Tutorials*; 2024 R2; ANSYS, Inc.: Canonsburg, PA, USA, 2024.
32. Pavlovic, A.; Fragassa, C.; Bertoldi, M.; Mikhnych, V. Thermal Behavior of Monocrystalline Silicon Solar Cells: A Numerical and Experimental Investigation on the Module Encapsulation Materials. *J. Appl. Comput. Mech.* **2021**, *7*, 1847–1855. [CrossRef]
33. Misha, S.; Abdullah, A.L.; Tamaldin, N.; Rosli, M.; Sachit, F. Simulation CFD and experimental investigation of PVT water system under natural Malaysian weather conditions. *Energy Rep.* **2020**, *6*, 28–44. [CrossRef]
34. Hocine, R.; Belkacemi, K.; Kheris, D. 3D-analytical method analysis of thermal effect in space shaded solar panel. In Proceedings of the 2019 9th International Conference on Recent Advances in Space Technologies (RAST), Istanbul, Turkey, 11–14 June 2019; pp. 339–344.
35. ANSYS, Inc. *Mechanical User's Guide*; 2024 R2; ANSYS, Inc.: Canonsburg, PA, USA, 2024.
36. Park, S.S.; Kim, Y.-J.; Kang, E.-C.; Lee, E.-J.; Entchev, E. Numerical investigations of a solar energy heat transfer performances with experimental validations in a water-based serpentine photovoltaic-thermal (PVT) collector. *J. Therm. Anal. Calorim.* **2023**, *148*, 2149–2169. [CrossRef]

Disclaimer/Publisher's Note: The statements, opinions and data contained in all publications are solely those of the individual author(s) and contributor(s) and not of MDPI and/or the editor(s). MDPI and/or the editor(s) disclaim responsibility for any injury to people or property resulting from any ideas, methods, instructions or products referred to in the content.